

# Effect of the Tool Geometries on Thermal Analysis of the Friction Stir Welding

Elhadj Raouache<sup>1</sup>, Zied Driss<sup>2,\*</sup>, Mohamed Guidara<sup>3</sup>, Fares Khalfallah<sup>4</sup>

<sup>1</sup>Civil Engineering Department, University, B.B.A–Algeria, Electronic Materials and Systems Laboratory, University, B.B A, Algeria

<sup>2</sup>Laboratory of Electro-Mechanic Systems (LASEM), National School of Engineers of Sfax (ENIS), University of Sfax, Sfax, Tunisia

<sup>3</sup>Laboratory of Mechanical Production and Materials (LGPM), National School of Engineers of Sfax (ENIS), University of Sfax, Sfax, Tunisia

<sup>4</sup>Department of Physical Engineering, University of M'sila, Algeria

**Abstract** In this paper, a three dimensional finite element was developed to study the transient thermal analysis of friction stir welding (FSW) for different tool geometries and different process parameters. The objective of this work is to investigate and analyze the temperature distribution of tool and work piece during operation using COMSOL MULTIPHYSICS. The model incorporates the mechanical reaction of the tool and the thermomechanical process of the welded material. The heat source incorporated in the model involves the friction between the material, the probe and the shoulder. The results obtained from the analysis are satisfactory compared with those the specialized literature.

**Keywords** Thermal analysis, Friction Stir Welding (FSW), Tool geometries, FE

## 1. Introduction

Friction stir welding (FSW) was invented at The Welding Institute (TWI) of UK in 1991 as a solid-state joining technique, and was initially applied to aluminum alloys [1]. The welds are created by the combined action of frictional heating and mechanical deformation due to a rotating tool [2].

A schematic diagram illustrating the process of FSW is shown in Figure 1. The key components of the FSW are:

- The shoulder: this is the primary means of generating heat during the process, prevents material expulsion and assists material movement around the tool.
- The pin: the pin's primary function is to deform the material around the tool and its secondary function is to generate heat [3].

In this context, Hamitton et al. [4] performed an analysis of thermal model of friction stir welding in aluminum alloys. The aim of this investigation was to introducing scaling factors that partitions the heat generation between plastic deformation and friction. Keivani et al. [5] studied the effect of pin angle and preheating on temperature distribution during friction stir welding operation. The authors studied the thermal characteristic of copper C11000 during the FSW process. This study provides better

understanding on the thermo-mechanical characteristics of weld material. Ulysse [6] presented a 3D finite element model for determining the temperature profile using a commercial FEM code FIDAP. The heat generation rate expressed as the product of the effective flow stress and the effective strain rate. Reasonable agreement between the predicted and the measured temperature was reported. Chen and Kovacevic [7] used a three-dimensional model based on finite element analysis to study the thermal history and thermo-mechanical process in the butt-welding of aluminum alloy 6061-T6. Their model was symmetry along the weld line and incorporated the mechanical reaction of the tool and thermo-mechanical process of the welded material.

The aim of the present work is to demonstrate the effect of different tool geometries and different process parameters on thermal analysis of FSW.

## 2. Material and Geometry

In this section, the strategy adopted for the numerical simulation of the FSW process is presented. First, it is important to choose the materials of work-piece. Secondly, it is interesting to choose the different geometries of tool. Typical values of the properties of this material are given in table 1 and table 2.

The tool geometries are illustrated in figure 2. They consist of four pin with different geometries. In the first case, we have adopted a cylindrical pin. However, we have used respectively two grooves, three grooves and four grooves, in

\* Corresponding author:

zied\_driss@yahoo.fr (Zied Driss)

Published online at <http://journal.sapub.org/mechanics>

Copyright © 2016 Scientific & Academic Publishing. All Rights Reserved

the second, the third and the fourth cases.

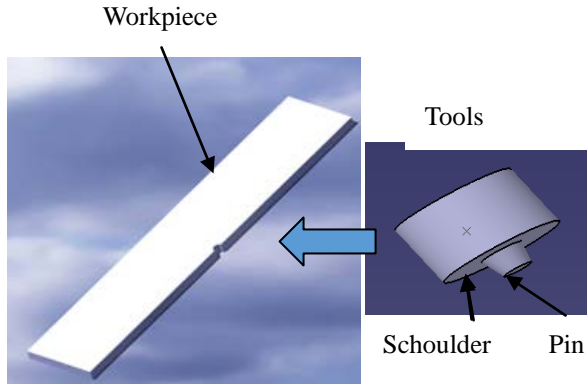


**Figure 1.** Schematic representation of Workpiece and tool

**Table 1.** Temperature dependence of the shear yield strength of aluminum 6061 alloy [8]

Temperature (°C)	311	339	366	394	422	450	477	533	589	644
Yield stress (MPa)	241	238	232	223	189	138	92	34	19	12

**Table 2.** Physical properties of aluminum 6061 alloy

Thermal conductivity	$K = 160 \text{ W/m.K}$
Density	$\rho = 2700 \text{ kg/m}^3$
Heat Capacity	$C_p = 900 \text{ J/kg.K}$

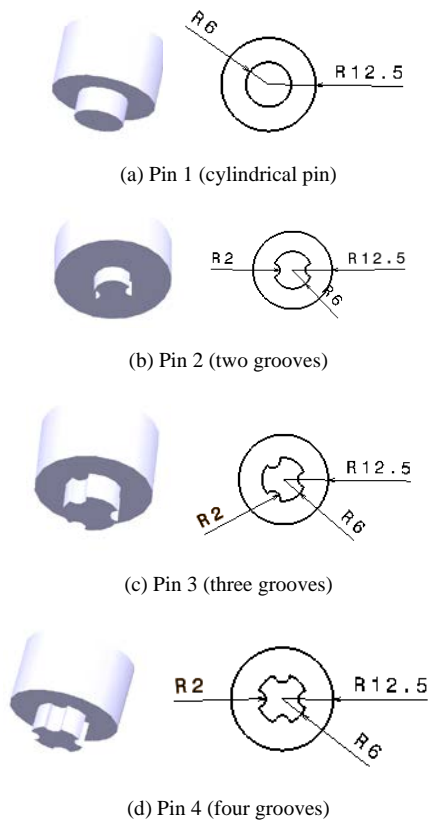


**Figure 2.** Different Tool Geometries

### 3. Boundary Conditions

The model dimensions are  $(350 \times 200 \times 6) \text{ m}$  in positive  $x$ ,  $y$  and  $z$  directions respectively. Aluminum alloy (AA6061-T6) is taken as the work piece due to its wide applications in the aerospace field because of its good formability, weldability, machinability, corrosion resistance and good strength compared to other aluminum alloys. Equation (1) describes the steady-state heat transfer in the plate where a convective term (right-hand side) is included to account for the effect of material movement.

$$\nabla \cdot (k \nabla T) + q = \rho C_p V_T \cdot \nabla T \quad (1)$$

$q$  represents the rate of heat source per volume;  $V_T$  is the welding (transverse) speed.

The model simulates the heat dissipation due to the interaction among the tool's pin and shoulder with the workpiece (surface heat of friction and volumetric heat of deformation) as a surface heat flux (space mapping) in the tool pin and shoulder (M.song *et al.*) [10]:

$$q_{\text{pin}}(T) = \begin{cases} \frac{\mu}{\sqrt{3(1+\mu^2)}} r_p \omega \bar{Y}(T) & : T < T_{\text{melt}} \\ 0 & : T > T_{\text{melt}} \end{cases} \quad (2)$$

$q$  ( $\text{W/m}^2$ ) is the pin heat flux and  $\mu$  is the friction coefficient between the pin and the workpiece,  $r_p$  denotes the pin radius,  $\omega$  refers to the pin's angular velocity ( $\text{rad/s}$ ), and  $\bar{Y}(T)$  is the average shear yield stress of the material as a function of temperature.

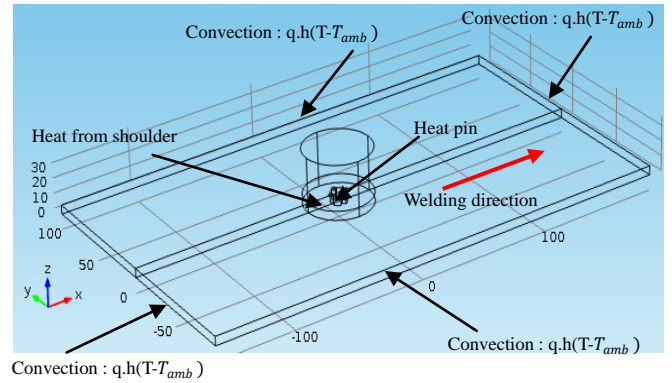


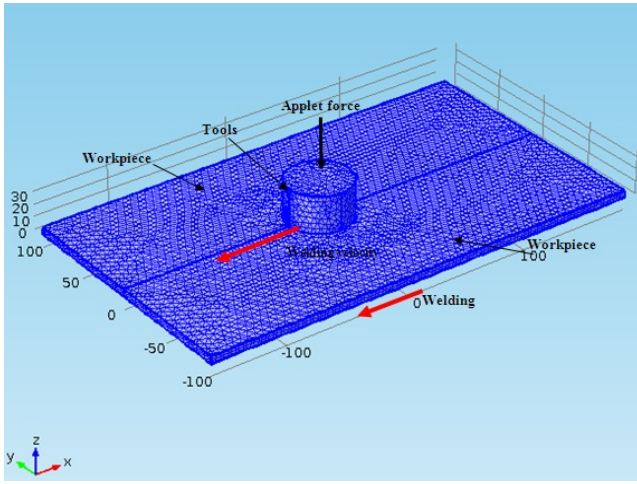
**Figure 3.** Boundary conditions in the presented heat transfer model

Meshing of the tool and workpiece has been done using Comsol Multiphysics. The element used for meshing has a tetrahedral shape (Figure 4).

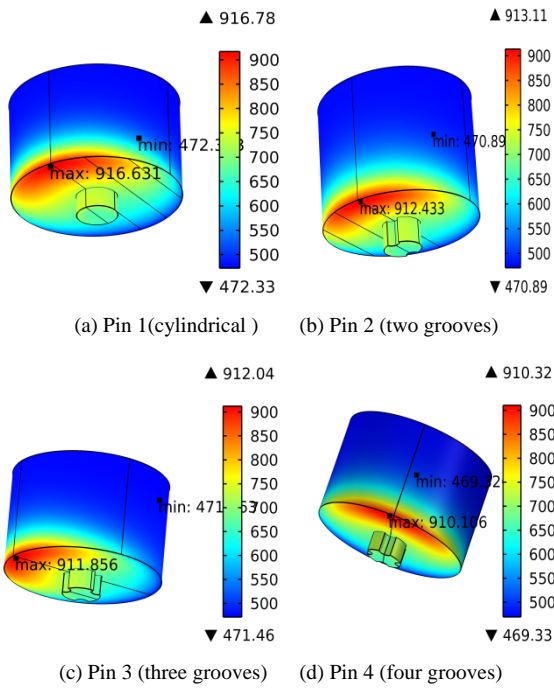
### 4. Results and Discussions

FSW welding process was modeled by Comsol Multiphysics to do a thermal analysis. Temperature distribution in tools resulting from the simulation of FSW is schematically shown in Figure 5. The welding conditions in this section are  $f_n=15 \text{ kN}$  and  $\omega=800 \text{ rpm}$ . According to these results, it is clear. That the maximum temperature is about  $T=916 \text{ K}$  in the cylindrical tool. This temperature does

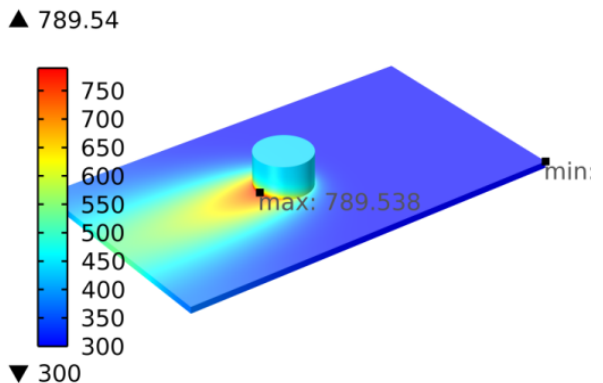
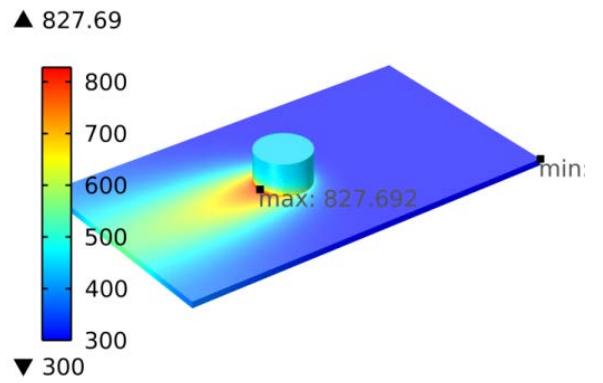
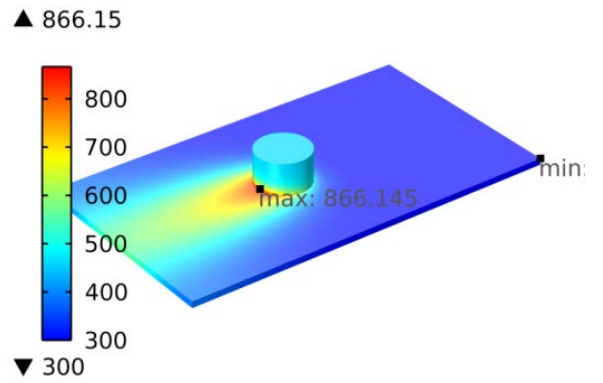
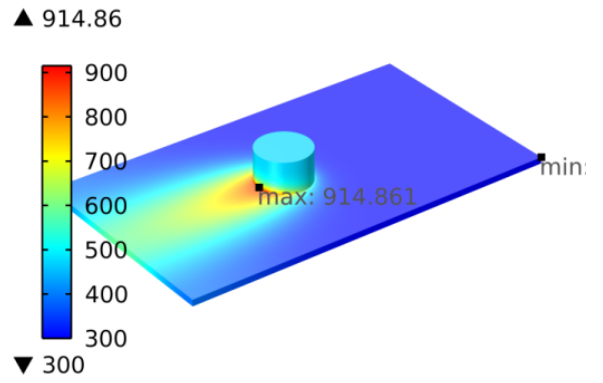
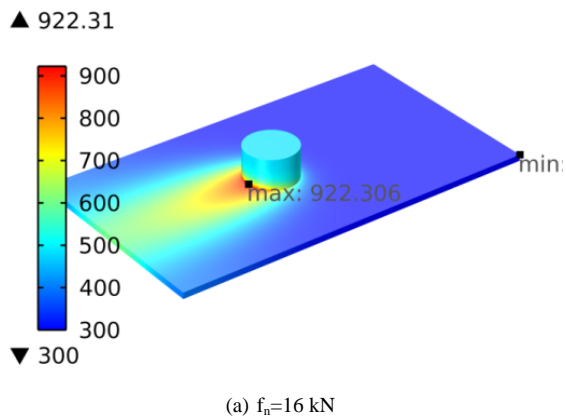
not exceed melting temperature of the alloy, equal to  $T=922$  K.



**Figure 4.** Meshed workpiece as well as tool utilized during simulation of friction stir welding



**Figure 5.** Comparison between the peak temperatures (3D view)



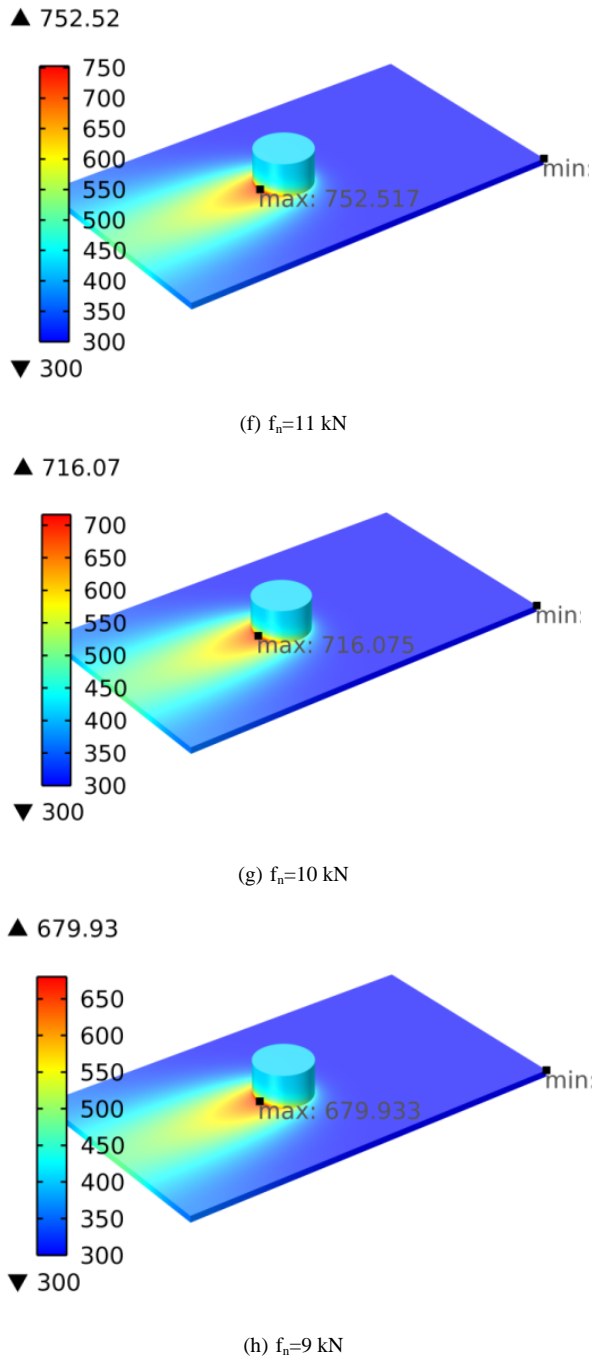


**Figure 6.** Temperature distributions obtained for different axial forces

#### 4.1. Effect of Axial Force

In this section, all results presenting the thermal distribution of the numerical model are presented and interpreted as well as those presented in the following sections were obtained from the following configuration welding:

- Different vertical forces equals to 9 kN, 10 kN, 11 kN, 12 kN, 13 kN, 14 kN, 15 kN and 16 kN,
- welding speed (9.5 mm/s) speed of 800 rpm,
- geometry Tool 4 (four grooves).

Figure 6 shows the temperature map in the plates during welding. According to these results, the temperature gradient is much higher than before the tool. The cooling plates are controlled by interaction with the external environment. Figure 7 shows the evolution of the temperature in the middle line of the assembled samples. This fact increases the penetration force leads to an increase of the maximum temperature. Figure 8 shows the maximum temperatures as function of axial force for a constant welding speed of 9.5 mm/s. Notice how the maximum temperatures stabilize for higher rotational speeds – being limited by the melting temperature of 922 K.

#### 4.2. Effect of the of Rotation Speed

To study the influence of rotation speed, we set the values of the forward speed of welding and the effort applied in this case, Figure 9 shows the variation of the maximum temperature in function of the rotation speed. According to these results, it is clear that the maximal temperature increases with the increase of the rotational speed as a linear function. It is clear that the maximum value  $T_{max}$  is obtained with a rotation of 800 rpm. These simulations were performed with the geometry 1, and confirm the results developed by Chiumenti [9].

#### 4.3. Effect of Feed Rate

In this section, the welding conditions are  $F_n = 15$  kN and  $\omega = 800$  rpm. Figure 10 shows the variation of the maximum temperature simulated as a function of the welding speed. According to these results, it has been noted that the maximum temperature decreases with the weldin speed as a linear function. The maximum value of the temperature is equal to  $T_{max} = 910$  K for a welding speed equal to  $V = 9.3$  mm/s.

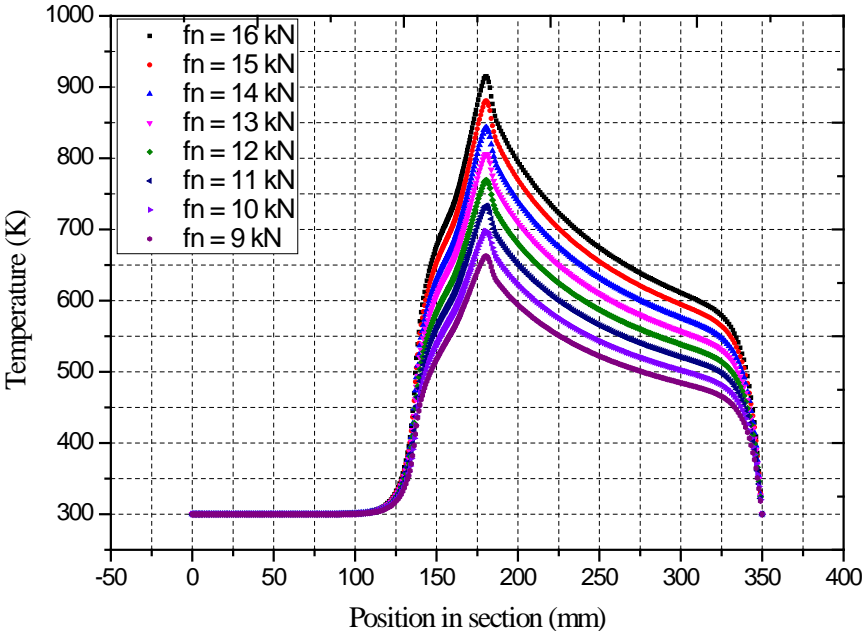


Figure 7. Line-graph of the temperature along the midsection for different axial force

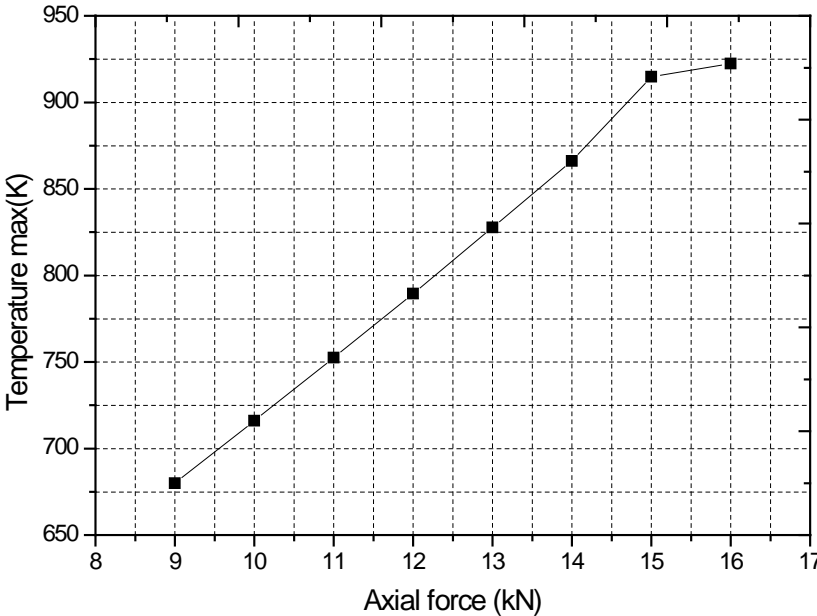


Figure 8. Variation of the maximum welding temperature at the stir-zone close to the pin

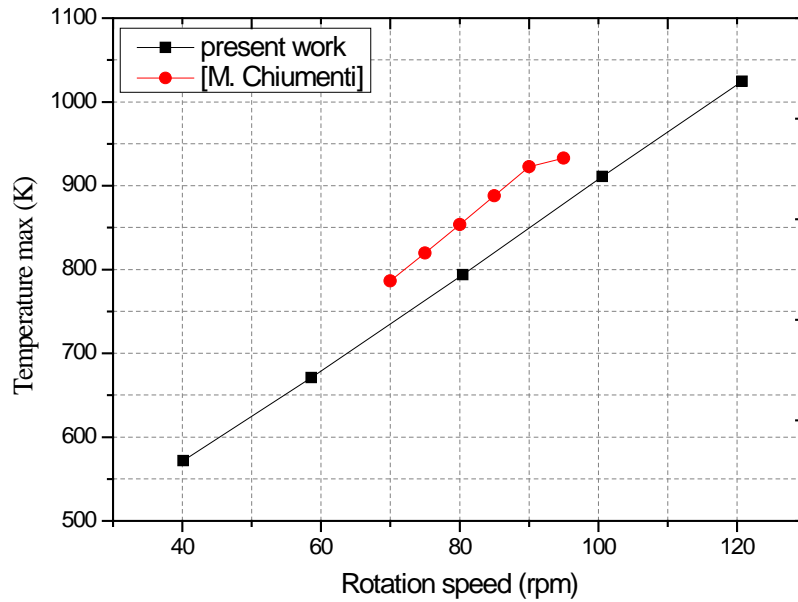


Figure 9. Variation of the maximum temperature in function of rotational speed

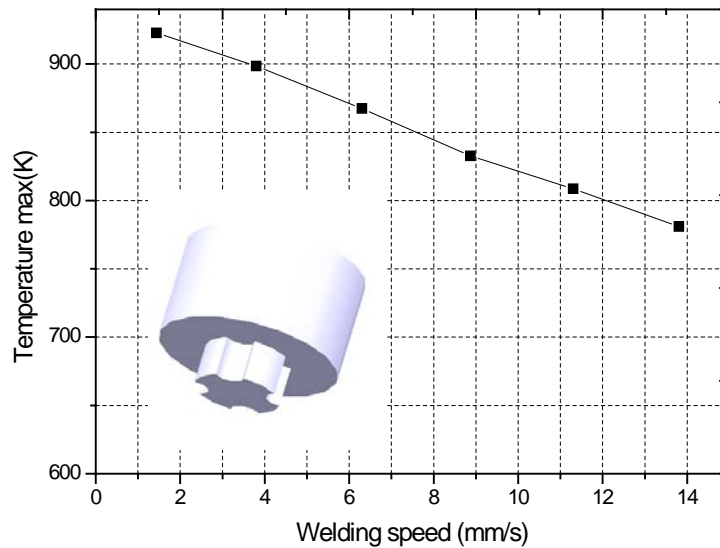


Figure 10. Effect of welding speed

## 5. Conclusions

In this paper, we have used the Comsol multiphysics code to investigate the thermal analysis in friction stir welds.

This study focused on the temperature variation reached during the movement of the welding material during the welding. The effect of the geometry of pin, as well as the speed of rotation of the tool, the penetration effort and the

forward speed has been studied. The comparison of the numerical results with the anterior results found in the literature confirms the validity of the numerical method. The results obtained in this paper are as follows:

- Tool probe geometry is very much responsible for deciding the weld quality.
- The maximum value of the temperature obtained near the weld increases as the tool holding time and rotational speed are increased.

---

## REFERENCES

- [1] R. Sharan Mishra, Partha Sarathi De Nilesh Kumar, 2014, Friction Stir Welding and Processing, ISBN 978-3-319-07042-1 ISBN 978-3-319-07043-8 (eBook), DOI 10.1007/978-3-319-07043-8, Springer Cham Heidelberg New York Dordrecht London.
- [2] P. Biswas and N.R. Mandal, 2011, Effect of tool geometries on thermal history of FSW of AA1100, Welding Journal July, 90.
- [3] Paul A. Colegrove, Hugh R. Shercliff, 2005, 3-Dimensional CFD modelling of flow round a threaded friction stir welding tool profile, journal of materials processing technology 169, 320-327.
- [4] C. Hamiton, S. Dymek, A. Sommers, 2008, A thermal model of friction stir welding in aluminum alloys. International journal of machine tools and manufacture, 48, 1120-1130.
- [5] R. Keivani, B. Bagheri, F. Sharifi, M. Ketabchi, M. Abbasi, 2013, Effects of pin angle and preheating on temperature distribution during friction stir welding operation, Transactions of Nonferrous Metals Society of China, 23(9), 2708-2713.
- [6] P. Ulysse, 2002, Three-Dimensional Modeling of Friction Stir-Welding Process, Int. J. Mach. Tools Manuf., 42, 1549-1557.
- [7] Chen CM. Kovacevic R. (2003).” Finite Element Modeling of Friction Stir Welding Thermal and Thermomechanical Analysis”. Int. J. Mach. Tools Manuf. 43:1319-1326.
- [8] Mohamadreza Nourani, Abbas S. Milani, Spiro Yannacopoulos, 2011, Taguchi Optimization of Process Parameters in Friction Stir Welding of 6061 Aluminum Alloy: A Review and Case Study, Engineering, 3, 144-155.
- [9] M. Chiumenti, 2013, Numerical modeling of friction stir welding processes, Comput. Methods Appl. Mech. Engrg. 254, 353-369.
- [10] M.song, R. Kovacevic, 2003, thermal modeling of friction stir welding in a moving coordinate system and its validation, international journal of machine tools and manufacture 43 (2003) 605-615.